Applied Physics A (2023) 129:320
https://doi.org/10.1007/s00339-023-06529-w

Applied Physics A
Materials Science & Processing

Hierarchical 'rose-petal' ZnO/Si surfaces with reversible wettability reaching complete water repellence without chemical modification

M. Kanidi[1] · A. Bardakas[2] · A. Kerasidou[2] · A. Anastasopoulos[1] · C. Tsamis[2] · M. Kandyla[1]

Received: 12 August 2022 / Accepted: 24 February 2023 / Published online: 4 April 2023

Abstract
Smart surfaces with externally controlled wettability patterns are ubiquitous building blocks for micro-/nanofluidic and lab-on-chip devices, among others. We develop hierarchical surfaces of ZnO nanorods grown on laser-microstructured silicon with reversible photo-induced and heat-induced wettability. The as-prepared surfaces are superhydrophilic, with very low water contact angles (~ 10°), and transition to a wetting state with high water contact angles (~ 150°) when annealed in vacuum. As the annealing temperature increases to 400 °C, the surfaces become completely water-repellent. Even though the annealed surfaces present high water contact angles, at the same time, they are very adhesive for water droplets, which do not roll off even when tilted at 90° or 180° (rose-petal effect), unlike standard hydrophobic surfaces which typically combine high water contact angles with low roll-off angles. The surfaces return to the superhydrophilic state when irradiated with UV light, which indicates a reversible wettability with external stimuli. Based on this transition, we demonstrate local modification of the wetting state of the surfaces by UV irradiation through a mask, which results in directed liquid motion, useful for microfluidic applications. The high contact angles obtained in this work are usually obtained only after chemical modification of the ZnO surface with organic coatings, which was not necessary for the hierarchical surfaces developed here, reducing the cost and processing steps of the fabrication route. These rose-petal surfaces can be used as "mechanical hands" in several applications, such as no-loss transport of small liquid volumes, precision coatings, spectroscopy, and others. Furthermore, the completely water-repellent surfaces, rarely reported elsewhere, may find important applications in frictionless liquid transport for microfluidic and other devices.

Keywords Reversible wettability · Annealing · UV irradiation · Rose petal effect · ZnO nanorods · Laser-microstructured silicon · Hierarchical adhesive surfaces · Water repellence

1 Introduction

Wettability is an important surface property, essential for many applications and products, such as paints, advanced textiles, water repellency, dirt removal, oil–water separation, programmable liquid transport, anti-biofouling, and smart soft robotics, among others [1, 2]. Furthermore, a surface with reversible wettability, switching between hydrophilicity and hydrophobicity, is required for rapid water motion, microfluidic devices, smart membranes, sensors, etc. [3]. A wettability switch can be triggered by various external stimuli, including electricity (based on electrowetting or the doping of conducting polymers) [4], temperature (based on thermoresponsive polymers) [5, 6], light (based on photosensitive metal-oxide semiconductors and photo-responsive organic compounds) [7], pH (based on protonation and deprotonation of pH-responsive surfaces) [8, 9], mechanical strain (based on extending and unloading elastic films) [10, 11], etc. Materials on which switching wettability has been demonstrated include polymers [2], metal oxides [12], silica [13], and magnetic nanoparticles [14], among others.

Metal oxides are usually photo-responsive, switching to a highly wetting state (hydrophilic) under ultraviolet (UV) illumination and returning to the original hydrophobic state after storage for sufficient time in the dark or via annealing [15]. Reversible wettability has been demonstrated

✉ M. Kandyla
kandyla@eie.gr

[1] Theoretical and Physical Chemistry Institute, National Hellenic Research Foundation, 48 Vasileos Constantinou Avenue, 11635 Athens, Greece

[2] Institute of Nanoscience and Nanotechnology, NCSR "Demokritos", 15310 Athens, Greece

in titanium dioxide (TiO_2), zinc oxide (ZnO), tin dioxide (SnO_2), tungsten trioxide (WO_3), vanadium pentoxide (V_2O_5), and others. This effect is based on the common mechanism of a switching surface chemical environment between two states, a hydrophilic one due to hydroxy groups on the surface and a hydrophobic one due to replacement of hydroxy groups by oxygen atoms [16, 17]. Among them, ZnO is a low-cost material with chemical and thermal stability, photocatalytic activity, and other useful physical and chemical properties, and it is actively used in the field of biomimetic surfaces [18–21]. ZnO micro/nano-structures, such as thin films, nanorods, nanowires, microholes, etc., have demonstrated reversible wettability, ranging from super-hydrophilicity to super-hydrophobicity, due to the combination of surface chemistry and morphology, useful for ultra-dry surfaces, self-cleaning, anti-fogging coatings, liquid transport, and others [22–25]. Incorporation of ZnO nano-structures onto functional surfaces can be achieved by a facile, 2-step chemical growth method, utilizing the deposition of an initial ZnO thin layer (seed layer) followed by the hydrothermal synthesis method. This chemical synthesis route offers a low-cost, low temperature, environmentally safe, and controllable method of developing ZnO nano-structures of various morphologies by tuning either the growth conditions or the seed layer properties [26, 27]. Because wetting properties can be tailored by manipulating the chemistry as well as the morphology of a surface, hierarchical ZnO-based surfaces have been employed to mimic natural hierarchical surfaces with extraordinary properties [12, 28–30]. Indeed, hierarchical surfaces of ZnO nanowires, flowers, thin films, nanopetals, and others, exhibited super-hydrophobicity for oil/water separation, corrosion resistance, etc.

Hydrophobic surfaces combine a high contact angle with water ($>90°$) and a low roll-off angle, which results in water droplets rolling off the surface even when this is slightly tilted. The roll-off angle of a surface is a characteristic parameter for many applications, where it is important to manipulate the mobility of water droplets. Hierarchically structured surfaces, however, can have either adhesive (high or no roll-off angle) or non-adhesive (low roll-off angle) properties while demonstrating a high contact angle. This depends on the wetting mode of the hierarchical surface, i.e., on the penetration of water into the macro- or nano-roughness, or into both [31]. The "lotus surface" shows a high contact angle and water droplets easily roll off, because air is trapped between the rough surface and water, as described by the Cassie model [32–34]. The "rose-petal surface" also shows a high contact angle, but water droplets stick to such a surface without rolling off, even at great tilt angles. Its wetting mechanism is described by the Wenzel model, indicating that a water droplet impregnates the roughness of the underlying surface, providing extended contact between them, and thus increased water adhesion and roll-off absence [35, 36]. Even though most studies on hydrophobic or superhydrophobic surfaces concentrate on lotus surfaces, some ZnO petal surfaces have been developed with ZnO hierarchical films, ZnO nanoparticles on micropatterned substrates modified with octadecylphosphonic acid, ZnO hexagonal nanorods on nanorod clusters, random networks of ZnO nanorods, ZnO nanorods modified with n-octadecanoic acid, etc. [30, 37–39]. In most cases, chemical modification of the surface with an organic coating is required, rendering these surfaces susceptible to mechanical and thermal instabilities.

In this work, we develop hierarchical "petal surfaces" of ZnO nanorods grown on laser-microstructured silicon substrates. Conical microstructures were created on a silicon wafer by irradiation with nanosecond laser pulses in an ambient of SF_6 gas, which is a common silicon etchant, in a process known as laser-assisted etching. ZnO nanorods were subsequently grown on the silicon microstructures by the hydrothermal method, to obtain hierarchical surfaces. The as-prepared surfaces are superhydrophilic and transition to a high contact angle wetting state when annealed in vacuum. As the annealing temperature increases, the surfaces become completely water-repellent, which is rarely reported, as shown in Table 1, and particularly useful for frictionless liquid transport in microfluidic and other devices with no fluid drag at water–solid interfaces. The annealed surfaces are very adhesive for water droplets, which do not roll off even when tilted at 90° or 180°. The high contact angles and petal effect obtained in this work are usually obtained only after chemical modification of the ZnO surface with organic coatings as mentioned earlier, which is not necessary for the hierarchical surfaces developed here. This reduces the cost and processing steps of the fabrication route to render it suitable for large-scale production and also increases the mechanical and thermal stability of the surfaces. The petal effect observed in this work arises as a result of the dimensions of the ZnO nanorods in relation to the dimensions of the silicon microstructure. The wettability is reversed to the superhydrophilic state when irradiating the surfaces with UV light, as in most metal oxides. We take advantage of this property, to induce local modification of the wetting state of the surfaces by UV irradiation through a mask, which results in directed liquid motion. Such smart surfaces with externally controlled wettability patterns are ubiquitous building blocks for controlled micro-/nanofluidic and lab-on-chip devices, where versatile manipulation of liquid motion is essential [40–42]. The rose-petal surfaces can be used as "mechanical hands" in several applications, such as no-loss transport of small liquid volumes, precision coatings, spectroscopy, and others [43].

Table 1 Summary of ZnO micro/nano-structures showing reversible wettability and comparison with this work

ZnO structure	Substrate	Hierarchical surface	Contact angle		Sliding angle	Chemical modification	Ref.
			Heat/Dark storage	UV irradiation			
nanorods	micro-Si	✓	150° – water repellent	10°	no sliding even upside down	no	this work
nanorods	flat Si		150°	--	--	no	[25]
film	micro-Si	✓	120° – 130°	~0°	--	no	[28]
film	micro-Si	✓	157°	30°	>90°	no	[29]
nanorods	flat Si		140°	--	--	no	[46]
microrods	glass		110°	20°	--	no	[51]
microholes	rough ZnO layer		150°	45°	--	no	[52]
micro/nano structured needles	stainless steel	✓	160°	~0° no UV, post-annealing	--	no	[23]
nanowire arrays	flat Si		160°	~0°	--	yes	[24]
microspheres with nanopetals	flat Si	✓	164°	--	3°	yes	[30]
nanostructured film	bamboo		160°	~0°	--	yes	[47]

2 Materials and methods

2.1 Laser-microstructured silicon substrates

Monocrystalline silicon wafers [(100), thickness 500 ± 25 μm, Active Business Company] were cleaned in an ultrasonic bath of acetone and methanol for 15 min each. Employing nanosecond laser processing, microstructured silicon substrates were structured in a gas environment of sulfur hexafluoride (SF_6) (Supplementary Information, Fig. S1). A pulsed Q-switched Nd:YAG laser system (Litron Lasers) was used with 1064 nm wavelength, 5 ns pulse duration, and 10 Hz repetition rate. A silicon wafer was placed in a vacuum chamber, which was evacuated to a base pressure of 10^{-2} mbar and filled with 0.6 bar SF_6. The laser beam was focused on the silicon wafer through a quartz window, using a lens of 20 cm focal length, to an average fluence of ~ 1 J/cm^2 on its surface. The vacuum chamber was raster-scanned with respect to the laser beam, using a computer-controlled set of *x*–*y* translation stages, with a scanning speed, such that each spot on the silicon surface was irradiated by 1000 laser pulses.

2.2 ZnO nanorods' growth: annealing conditions

ZnO nanorods were grown on flat and microstructured silicon substrates using the hydrothermal method. A sol–gel-derived seeding layer was deposited on the silicon samples to facilitate nanorod growth. Zinc acetate dihydrate ($Zn(CH_3COO)_2\ 2H_2O$, Merck) was dissolved in ethanol absolute (VWR) at a concentration of 40 mM and the sol–gel solution was magnetically stirred for 1 h at 60 ℃. After the solution had reached room temperature, it was spin-coated on top of the samples at 1000 rpm and then annealed at 500 ℃ for 10 min on a hotplate. The spin-coating/annealing cycle was repeated ten times resulting in a thin ZnO film. The hydrothermal growth of ZnO nanorods was performed in an equimolar solution of zinc nitrate hexahydrate [$Zn\ (NO_3)_2\ 6H_2O$] (Sigma) and hexamethylenetetramine (HMTA) [$(CH_2)_6N_4$] (PanReac) at a concentration of 40 mM. The nutrient solution was prepared by dissolving the precursors in 700 ml of deionized (DI) water with the aid of magnetic steering. The seeded samples were placed upside down inside the growth solution for 1 h at a constant temperature of 87 ℃. The samples were finally removed from the solution, rinsed thoroughly with DI water and dried on a hotplate at 80 ℃ (Supplementary Information, Fig. S6). The as-grown samples were placed in a vacuum chamber and annealed at different temperatures to examine the reversibility of the wetting state. The vacuum chamber was pumped down using a turbomolecular pump at a base pressure of ~ 10^{-6} mbar and annealing of the samples was performed by a temperature-controlled silicon carbide heater at 200, 300, and 400 ℃ for 2 h. The samples were left to cool at room temperature in vacuum, and afterwards, the chamber was purged with N_2. The samples were removed from the chamber and were immediately stored in a vacuum-sealed and light-proof container.

2.3 UV irradiation

ZnO nanorods, grown on flat and microstructured silicon substrates, were irradiated by a low-pressure Hg UV lamp (Hanovia Ltd.), which mainly emits light centered at 254 nm, with an irradiance of ~ 3 mW/cm^2 for 6 and 12 h. The irradiation time was determined by the sample response and preceded contact angle measurements.

2.4 Characterization

The samples were characterized by scanning electron microscopy (SEM), using a field-emission microscope (JEOL 6301F), also equipped with energy-dispersive X-ray spectroscopy (EDS). No preparation was required and the samples were used as grown. SEM images were obtained either at 45° or at cross-sectional view. All images were obtained by secondary electron imaging (SEI). For 45° images, 15–25 kV were employed with working distances in the range 7.4–10.8 mm, while for cross-sectional views, 2.0–2.5 kV with working distances in the range 2.3–3.0 mm. The SEM images were analyzed with the software ImageJ, for the extraction of geometrical characteristics of the samples. EDS images and spectra were recorded on as-grown samples without additional preparation, simultaneously with the SEM measurements.

2.5 Contact angle measurements

A water droplet of 5 μL (distilled water) was deposited on the surface of each sample to measure the contact angle (CA) at room temperature (25 °C). Images and videos of water droplets on the surface were obtained by a 2.0MP 500× USB Digital Microscope. Images were extracted from videos and analyzed by standard MATLAB functions, transforming them to grayscale and determining subsequently the droplet edge profile. The profile was numerically analyzed in polar coordinates (r, θ) and the origin of the coordinates was chosen on the intersection between the apparent perpendicular axis of symmetry of the droplet and the solid/liquid interface. The profiles $r(\theta)$ obtained this way vary smoothly with θ and were easily modelled by fourth-order polynomials. The contact angles were extracted from the derivatives

on the left- and right-side contacts of the droplet with the surface and transformed back to Cartesian coordinates. Typically, the deviation between left and right contact angles was less than 2º. The average of the two values is considered as the contact angle of the droplet. For each sample, water contact angles were measured three times, and independent duplicate samples were prepared and measured for each reported contact angle.

3 Results and discussion

Scanning electron micrographs (SEM) of ZnO nanorods, grown on flat silicon, are presented at an angle of 45° (Fig. 1a) and in cross-sectional view (Fig. 1b). The average height of ZnO nanorods is 630 ± 36 nm, while the average diameter is 49 ± 9 nm (measurements shown in Supplementary Information, Fig. S2). We observe the silicon substrate is completely covered by ZnO nanorods and there are no void areas after their growth. ZnO nanorods are grown almost vertically and homogeneously on the silicon substrate, inducing nano-roughness on the surface. The hydrothermal technique is a wet chemical fabrication method with good experimental reproducibility that allows uniform growth of ZnO nanorod arrays at a large scale [24]. Moreover, the ZnO morphological characteristics, such as diameter and length, can be controlled by varying experimental parameters, such as the growth temperature, pH, and zinc seed layer morphology [44].

Contact angle measurements on the ZnO nanorods are shown in Fig. 2a. For these measurements, ZnO nanorods are used either as-grown, or after annealing in vacuum at 300 °C, or after UV irradiation for 6 h, to switch the ZnO wetting behavior. Two consecutive cycles of annealing-UV irradiation are shown in Fig. 2a. The contact angle of as-grown ZnO nanorods on flat silicon is very low (~ 10°), indicating super-hydrophilicity. This observation is attributed to hydroxy groups that are created on the surface of ZnO nanorods during synthesis [3]. Indeed, it is established that the wettability of metal oxides in general switches between hydrophilicity and hydrophobicity, depending on the presence of hydroxy groups on their surface [45]. For ZnO in particular, it has been shown that surface hydroxy groups

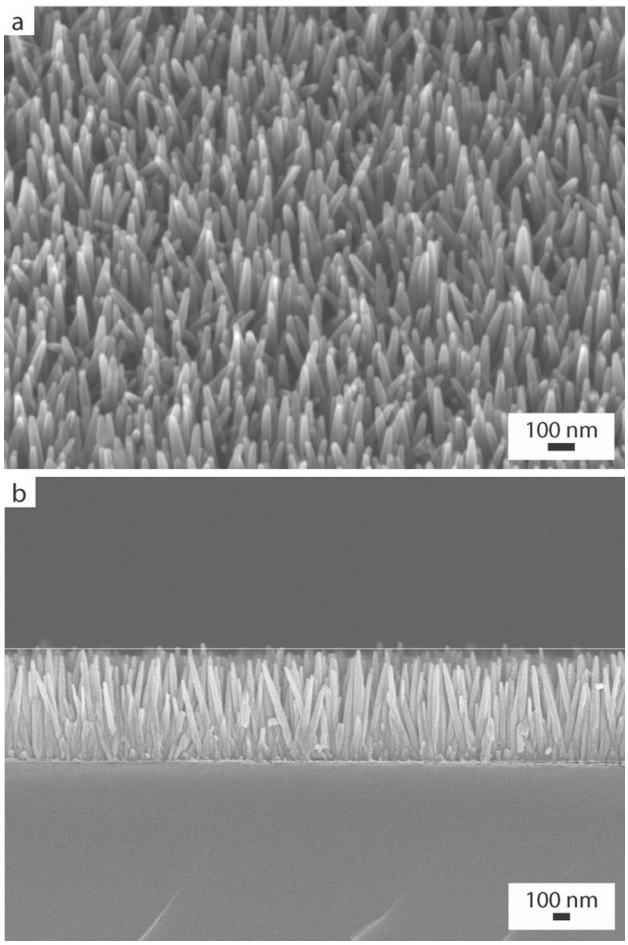

Fig. 1 SEM images of ZnO nanorods grown on flat silicon at **a** side (45°) and **b** cross-section view

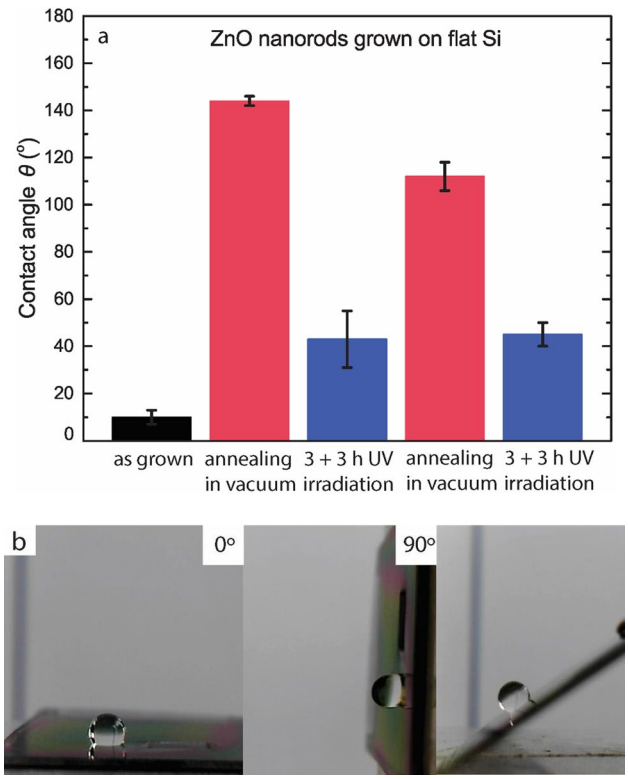

Fig. 2 **a** Water contact angle measurements on ZnO nanorods, as-grown on flat silicon, after annealing for 2 h at 300 °C in vacuum, and after UV irradiation twice, for 3 h each time. **b** Images of a water droplet, deposited on annealed ZnO nanorods on flat silicon, tilted at 0°, 90°, and at a random angle

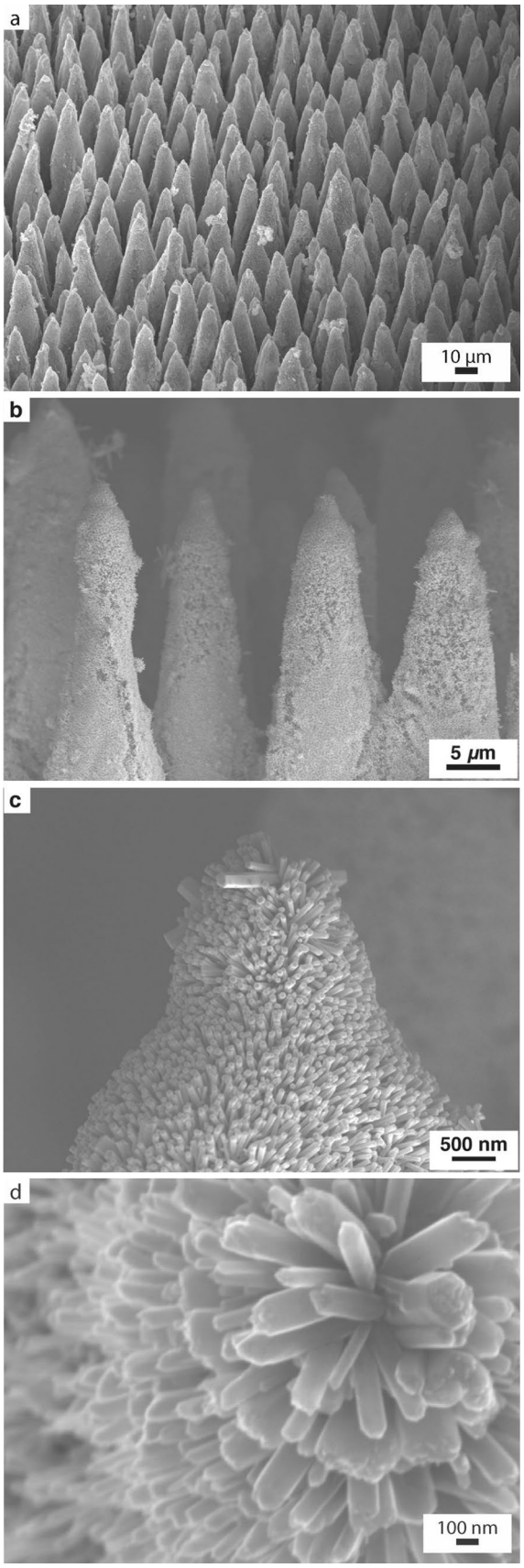

Fig. 3 SEM images of ZnO nanorods grown on microstructured silicon at **a**, side (45°) **b**, **c**, cross section, and **d** top view ►

render it hydrophilic for various synthesis and growth methods, indicating this is a property of the material itself, rather than a consequence of the synthesis or growth conditions [22–25, 28]. After annealing at 300 °C, the contact angle of ZnO nanorods is ~ 140°, indicating hydrophobicity. Annealing, and specifically annealing in vacuum, can accelerate the elimination of the surface hydroxy groups, thus converting the hydrophilic surface to a hydrophobic one [23, 46]. To reverse the ZnO wetting behavior back to the initial state, the ZnO nanorods were initially irradiated with UV light for 3 h, but no significant difference was observed in their wetting behavior. For this reason, the UV irradiation was repeated for 3 more hours, resulting in 6 h of total irradiation. After 6 h of UV irradiation, the contact angle shows a decrease of ~ 100°, indicating a switch to hydrophilicity. Even though a significant decrease of the contact angle is observed upon UV irradiation, the ZnO nanorods do not reach their initial state of super-hydrophilicity (CA ~ 10°), which would probably require a longer UV exposure. This photo-responsive behavior is common for various metal oxides, as mentioned in the Introduction. Upon UV irradiation, electron–hole pairs are formed in the lattice of ZnO. Some of the holes form surface oxygen vacancies, while the electrons form defect sites, which are kinetically more favorable for hydroxy adsorption than oxygen adsorption, enhancing the surface hydrophilicity [3]. To reverse the photo-induced effect, it has been demonstrated that oxygen atoms gradually replace the hydroxy groups adsorbed on the defect sites, resulting in surface hydrophobicity, when a sample is placed in the dark or annealed in vacuum after UV irradiation [23, 46, 47]. Indeed, repeating a second cycle of annealing/irradiation, a reversible wetting behavior is observed for the ZnO nanorods, switching between hydrophilicity and hydrophobicity (Fig. 2a).

Images of a water droplet on ZnO nanorods at 0°, 90°, and at a random tilting angle, measured after annealing in vacuum at 300 °C, are presented in Fig. 2b. On the annealed hydrophobic ZnO surface, the water droplet did not slide even when the samples were turned upside down at 180°, indicating a sticky hydrophobic ZnO surface (tilting the ZnO surface from 0° to 90° in video S1, Supplementary Information). Such a behavior can be attributed to a "petal surface", as described in the Introduction, where the nano-rough surface is getting wet, providing extended contact between water and the ZnO nanorods, and thus increased adhesion and roll-off absence.

As a next step, we developed hierarchical surfaces, combining micro- and nano-morphology, by growing ZnO nanorods on laser-processed silicon microstructures,

as shown in Fig. 3. The silicon surface is covered by conical microstructures with a mean half-height diameter of 15 ± 2 μm, a mean height of 65 ± 5 μm, and a mean distance between neighboring microstructures of 16 ± 3 μm center-to-center (Fig. 3a). Nanosecond laser irradiation of silicon in SF_6 environment results in the formation of such microstructures due to melting and interference effects [5]. Tuning the fabrication parameters, such as the laser wavelength, pulse duration, fluence (J/cm^2), number of pulses, the gas or liquid environment, and its pressure, we are able to control the surface morphology [48, 49]. The ZnO nanorods were grown on microstructured silicon, covering entirely the microstructures (Fig. 3b). Although it is difficult to measure the dimensions of ZnO nanorods grown on this substrate, we observe that ZnO nanorods were grown vertically to the non-planar substrate (Figs. 3c,d) similar to the growth direction of ZnO nanorods on flat silicon (Fig. 1b). To verify the spatial distribution of ZnO nanorods on the microstructured silicon substrate, an EDS elemental analysis is presented in Fig. 4. The EDS spectrum of ZnO nanorods on microstructured silicon shows Zn, Si, and O peaks (Fig. 4a). Mapping analysis and layered images show the detected elements and their distribution on the surface (Fig. 4b). The elements of zinc and oxygen correspond to the presence of ZnO nanorods and they are detected on the entire surface, verifying that ZnO nanorods cover the silicon microstructures, as well as the valleys between them.

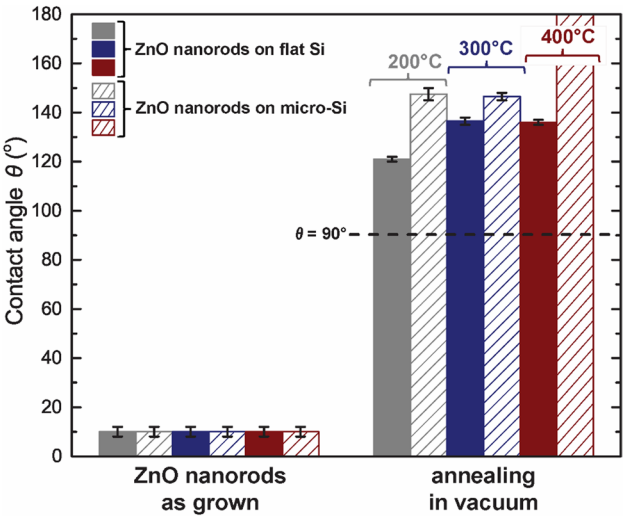

Fig. 5 Water contact angle measurements on ZnO nanorods, grown on flat and microstructured silicon, as-grown and after annealing for 2 h in vacuum at three different temperatures. The contact angle of ZnO/micro-Si annealed at 400 °C is only indicatively shown as ~ 180°, because in reality this surface is completely water-repellent

In Fig. 5, we study the effect of annealing temperature on the wetting behavior of ZnO nanorods on flat and microstructured silicon. Contact angle measurements are presented for as-grown samples and samples annealed for 2 h in vacuum at three different temperatures (200, 300, and

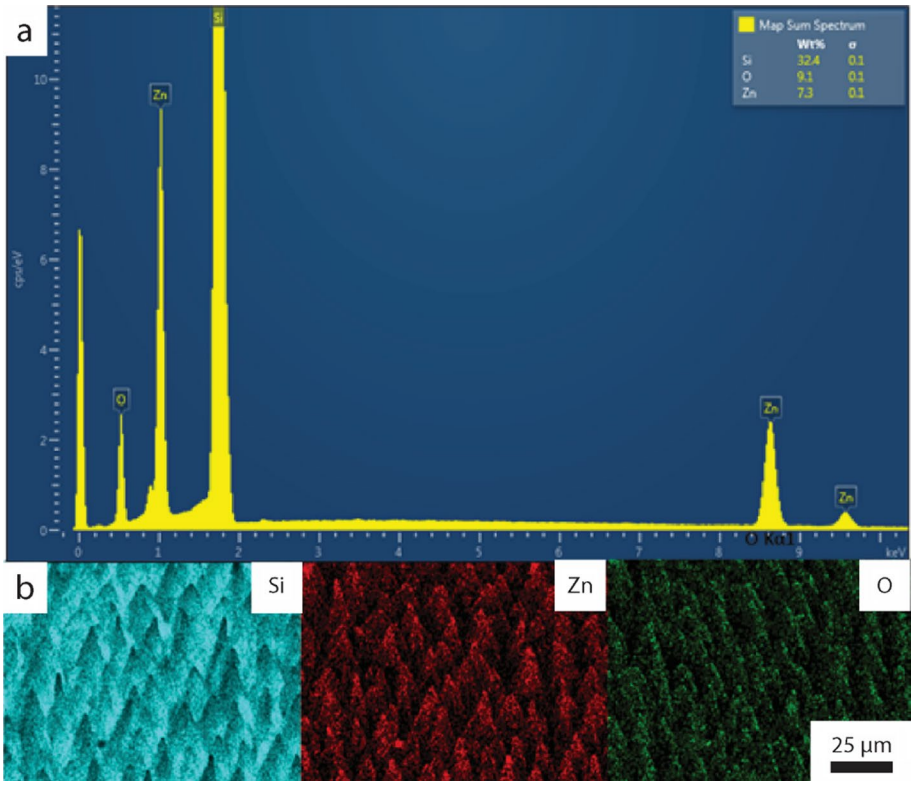

Fig. 4 **a** EDS analysis of ZnO nanorods grown on microstructured silicon substrate and **b** mapping distribution of elements

400 °C). As-grown ZnO nanorods present a similar superhydrophilic behavior either on flat or microstructured silicon. After annealing in vacuum, all samples present an increase in their contact angle, switching to hydrophobicity. However, the hierarchical surfaces (ZnO nanorods/micro-Si) present a higher increase of the contact angle for all annealing temperatures, resulting in a pronounced hydrophobic state. Especially for the samples annealed at 400 °C, the water droplet was completely repelled from the surface, preferring the pipette surface (Fig. 6b and video S4b in Supplementary Information). Therefore, the contact angle of these samples is only indicatively shown as ~ 180° in Fig. 5. There are several scenarios that describe the wetting of a surface with hierarchical roughness, which is quite complex [31, 43, 50]. Microstructuring of silicon enhances the ZnO nanorod responsiveness to annealing due to the large specific area of the hierarchical surface, which allows extended contact between water and the ZnO nanorods. Thus, the wetting behavior of ZnO nanorods grown on microstructured silicon is described by the Wenzel model. The temperature of thermal annealing is a crucial factor for ZnO wettability and several studies have focused on the temperature range 200–800 °C in vacuum or air, reporting a hydrophobic state up to a certain temperature, which then switches to a

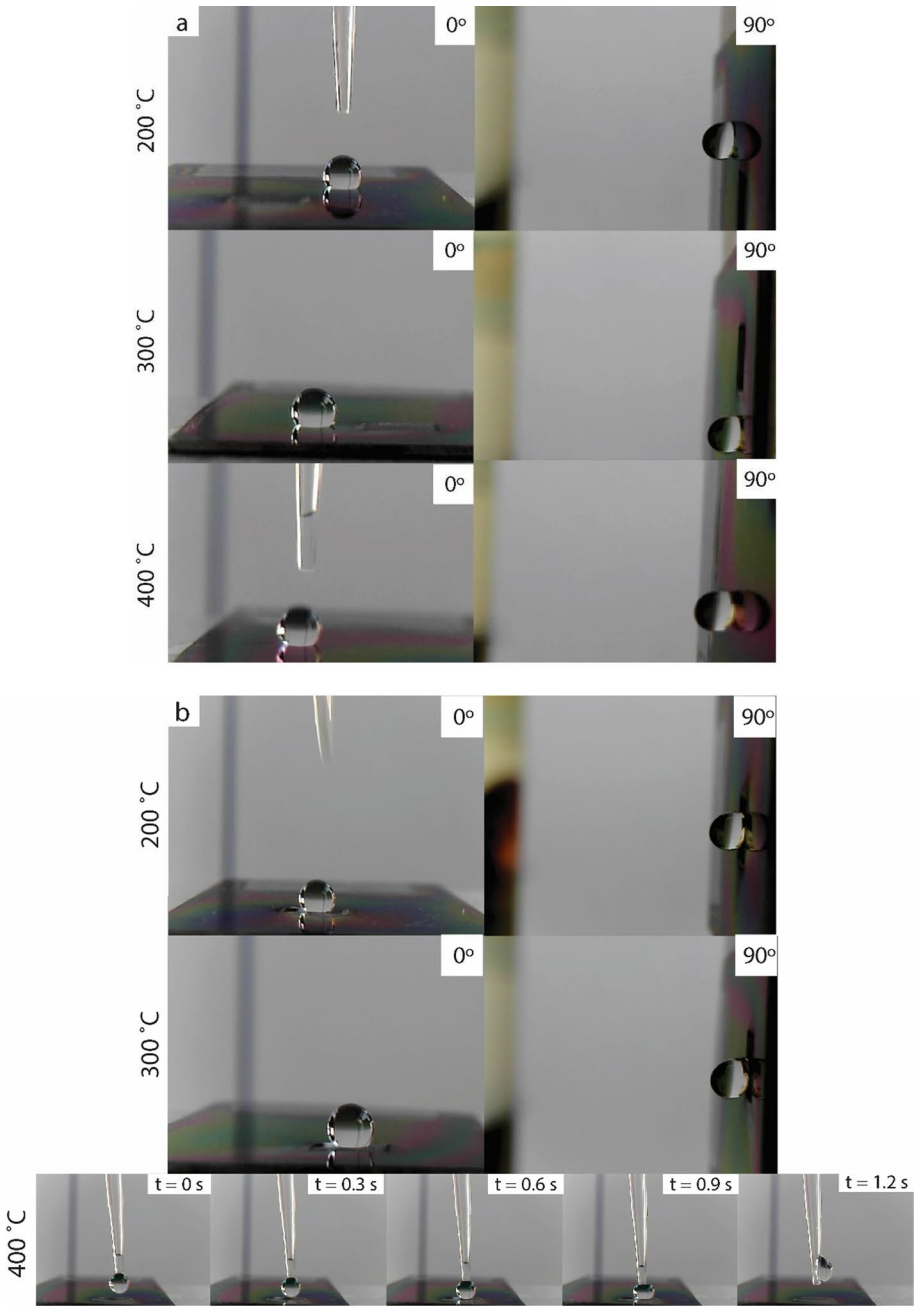

Fig. 6 Images of a water droplet deposited on ZnO nanorods, grown on **a** flat and **b** microstructured silicon and annealed for 2 h in vacuum at 200 °C, 300 °C, and 400 °C, tilted at 0° and 90°. Sequence of images of water droplet deposition on ZnO nanorods on microstructured silicon, annealed at 400 °C, demonstrates that the surface is completely water-repellent

hydrophilic state when the temperature is further increased [23, 25, 46, 51]. The effect of annealing persists for days, as shown in Fig. S5 in Supplementary Information. We measured the contact angle on hierarchical ZnO nanorod/micro-Si samples, annealed for 2 h in vacuum at 200 and 300 °C, for a time interval of 7 days. We observe that the contact angle remains practically the same for both samples, indicating that surface oxidation does not produce observable effects during this interval.

Images of a water droplet on ZnO nanorods, grown on flat and microstructured silicon (tilted at 0° and 90°), are shown in Fig. 6a, b, respectively. The samples are annealed for 2 h in vacuum at 200, 300, and 400 °C. All ZnO surfaces are sticky with a high contact angle and the water droplet preserves its shape even when tilted at 90° (more pictures of samples tilted at random angles are shown in Figs. S3 and S4). This behavior can be explained by the "rose petal effect", according to which extended contact area between water and the ZnO nanorods leads to increased water adhesion on the surface [29–31]. The conical shape and the size of the silicon microstructure and the shape and size of the ZnO nanorods render this surface a "rose petal" one, instead of a "lotus" one, which typically has a columnar microstructure and a needle-shaped nanostructure with smaller sizes [43, 50]. No water droplet images exist at 90° for the ZnO nanorod/micro-Si surface annealed at 400 °C, because it is not possible to deposit a water droplet on this surface on a typical attempt of 1.2 s duration (Fig. 6b). During this time, the ZnO/Si hierarchical surface is not impregnated with the water droplet probably due to lack of residence time [50]. Despite numerous studies, the adhesion mechanisms of hydrophobic surfaces and the wetting mechanisms of hierarchical surfaces are not yet completely understood; thus, there are several hypotheses to comprehend these mechanisms [3].

To investigate the reversibility of the wetting state of the hierarchical surfaces, ZnO nanorods on microstructured silicon were irradiated for 6 and 12 h with UV light after annealing and their contact angles are presented in Fig. 7, in comparison with the contact angles of ZnO nanorods grown on flat silicon. After 6 continuous hours of UV irradiation, ZnO nanorods grown on flat silicon reverse their wetting behavior to the initial state of super-hydrophilicity, while the ZnO nanorods grown on microstructured silicon remain hydrophobic, even though they present a decrease in their contact angles. Specifically, ZnO/Si hierarchical surfaces, previously annealed at 200 °C and 400 °C, present a decrease in contact angle of ~ 30° after 6 h of UV irradiation, preserving contact angles > 90°. Only for ZnO/Si hierarchical surfaces previously annealed at 300 °C, a decrease in contact angle of ~ 40° is present after 6 h of UV irradiation, approaching a contact angle of ~ 90°, close to a reversal of the wetting behavior towards hydrophilicity. Instead, the ZnO/Si hierarchical surfaces require more time

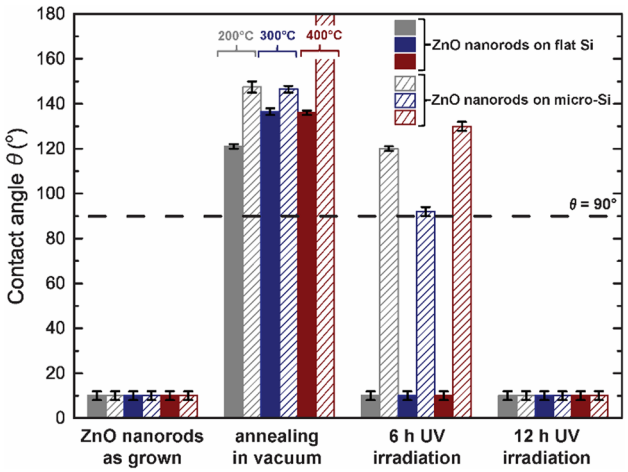

Fig. 7 Water contact angle measurements on ZnO nanorods, as-grown on flat and microstructured silicon substrates, after annealing for 2 h in vacuum, and after 6 and 12 h of UV irradiation. The contact angle of the ZnO/micro-Si sample annealed at 400 °C is only indicatively shown as ~ 180°, because in reality, this surface is completely water-repellent

(12 h) of UV irradiation to reverse their wetting behavior to the initial superhydrophilic state. This fact is attributed to the higher contact angles that are measured on ZnO nanorods grown on microstructured silicon after annealing. The hierarchical ZnO/Si surfaces are more hydrophobic than the surfaces of ZnO nanorods on flat silicon after annealing; thus, the hierarchical surfaces require longer UV irradiation to switch to the hydrophilic state. A similar reversible wetting behavior has been reported for other hierarchical ZnO structures, however, without reaching a completely water-repellent state [12, 28, 29, 52]. Table 1 summarizes the results of this work in comparison with other ZnO micro/nano-structures on various substrates, showing a reversible wettability. The high contact angles obtained in this work are usually obtained only after chemical modification of the ZnO surface with organic coatings. However, the hierarchical structure developed here induces similarly high contact angles after annealing, without chemical modification, and reaches a completely water-repellent state, which is rarely reported.

By taking advantage of the reversible wettability of the surfaces, we are able to locally modify their wetting state for directed liquid motion. To this end, we irradiated annealed hydrophobic ZnO nanorod surfaces, either on flat or microstructured silicon, by UV light using a mask, to create a UV-irradiated area only on half of the surface (as indicated in Fig. 8). Both wetting states of the ZnO surface, the hydrophobic and hydrophilic one, can be observed in Fig. 8a. An image of two water droplets, one on the irradiated and one on the non-irradiated area of annealed ZnO nanorods grown on flat silicon, shows

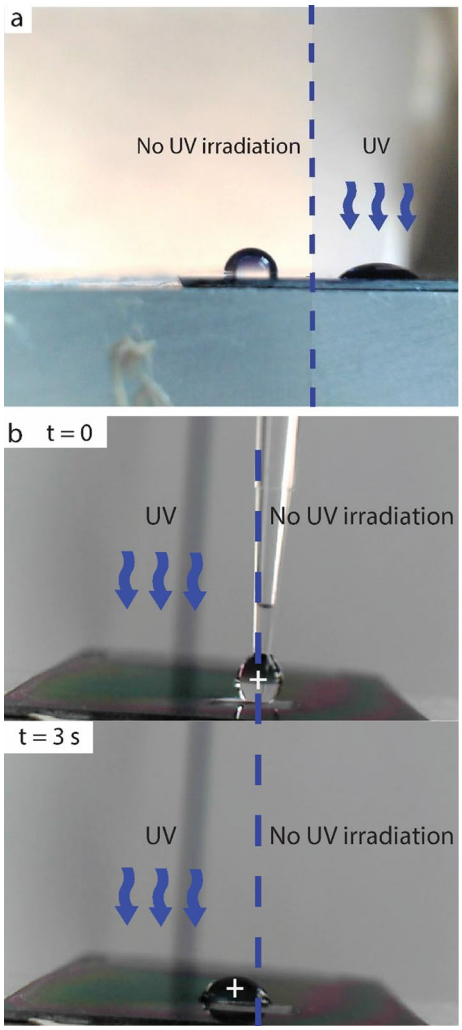

Fig. 8 **a** Image of two water droplets, on the non-irradiated area (left) and the UV-irradiated area (right) of ZnO nanorods grown on flat silicon, annealed for 2 h in vacuum at 300 °C. **b** Images of a water droplet deposited on ZnO nanorods grown on microstructured silicon, annealed for 2 h at 300 °C, at $t=0$ and $t=3$ s. The dashed line indicates the border between the irradiated and non-irradiated areas. The cross indicates the mass center of the water droplet

that the non-irradiated area remains hydrophobic, while the UV-irradiated area has become hydrophilic. Therefore, we can create a smart surface with areas of different wetting states that can be controlled by the stimulus of UV light. Following a similar procedure, a hierarchical surface of ZnO nanorods on microstructured silicon, annealed in vacuum for 2 h at 300 °C, was half-irradiated by UV light using a mask (as indicated in Fig. 8b). A water droplet was deposited on the border between the irradiated and non-irradiated areas. Figure 8b shows images of the droplet at the moment of deposition ($t=0$) and 3 s later (video S6 in Supplementary Information). Although the water droplet was initially deposited on the border between the two areas, it moved towards the UV-irradiated area after 3 s, where it spread. This is attributed to the hydrophilic state of the UV-irradiated area, which is preferable for the water droplet, compared to the hydrophobic non-irradiated area. Therefore, we can direct the motion of a water droplet by controlling the wetting state of a surface locally via UV irradiation. Such effective anisotropic wetting and the resulting spontaneous motion of liquids can be useful for microfluidic applications [40–42, 53, 54].

4 Conclusions

We developed hierarchical surfaces of ZnO nanorods grown on laser-microstructured silicon with photo-induced and heat-induced wettability. The as-prepared surfaces are superhydrophilic and become hydrophobic after annealing in vacuum. The wetting state of ZnO nanorods switches reversibly to a hydrophilic one upon UV irradiation due to electron–hole pairs formed in the lattice of ZnO. The annealing effect is significantly more pronounced on the hierarchical ZnO nanorod/micro-Si surfaces, compared with control surfaces of ZnO nanorods grown on flat silicon, due to the large specific area of the hierarchical structure, which enhances the sample responsiveness to temperature. Especially when annealed at 400 °C, the hierarchical ZnO/Si surface becomes completely water repellent, which is useful for frictionless liquid transport in microfluidic and other devices. The hierarchical surfaces require longer UV exposure to switch back to the hydrophilic state after annealing, compared with the control surfaces. Even though the annealed surfaces show high contact angles, they are very adhesive and water droplets do not roll off even when tilted at 90° or 180°, which is explained by the "rose petal" effect. Such surfaces can be used as "mechanical hands" for no-loss transport of small liquid volumes, precision coatings, spectroscopy, etc. Local modification of the wetting state is achieved using a mask during UV irradiation to expose only parts of the surface to UV light. This way, we develop smart surfaces, which can direct the motion of liquids from hydrophobic to hydrophilic areas of the surface. Furthermore, the effect is reversible as we can "erase" the hydrophilic areas by annealing the samples and create new ones by local UV irradiation, rendering these surfaces reusable for various applications. Such smart surfaces that respond to external stimuli reversing their wetting behavior pave the way for applications that require wettability control and manipulation of liquid mobility using advanced materials with novel properties at the micro- and nanoscale.

Supplementary Information The online version contains supplementary material available at https://doi.org/10.1007/s00339-023-06529-w.

Acknowledgements We acknowledge support of this work by the project "Advanced Materials and Devices" (MIS 5002409) which is implemented under the "Action for the Strategic Development on the Research and Technological Sector", funded by the Operational Programme "Competitiveness, Entrepreneurship and Innovation" (NSRF 2014-2020) and co-financed by Greece and the European Union (European Regional Development Fund). We also thank Dr. C. Chochos and M.C. Skoulikidou for their help with SEM and EDS measurements, Dr. A. Papagiannopoulos for his help with contact angle measurements, and Dr. A. Kaidatzis for his help with annealing the samples under vacuum.

Funding Open access funding provided by HEAL-Link Greece.

Data availability Data of this study are available from the corresponding author on reasonable request.

References

1. M. Sharma, K. Khare, Smart surfaces with tunable wettability, in 21st century surface science—a handbook. London, United Kingdom: IntechOpen, 2020.
2. Z. Pan, F. Cheng, B. Zhao, Bio-inspired polymeric structures with special wettability and their applications: an overview. Polymers **9**, 725 (2017)
3. W. Li, Y. Zhan, A. Amirfazli, A.R. Siddiqui, S. Yu, Recent progress in stimulus-responsive superhydrophobic surfaces. Prog. Org. Coat. **168**, 106877 (2022)
4. P. Teng, D. Tian, H. Fu, S. Wang, Recent progress of electrowetting for droplet manipulation. Mater. Chem. Front. **4**, 140–154 (2020)
5. M. Kanidi, A. Papagiannopoulos, A. Matei, M. Dinescu, S. Pispas, M. Kandyla, Functional surfaces of laser-microstructured silicon coated with thermoresponsive PS/PNIPAM polymer blends: switching reversibly between hydrophilicity and hydrophobicity. Appl. Surf. Sci. **527**, 146841 (2020)
6. M. Kanidi, A. Papagiannopoulos, A. Skandalis, M. Kandyla, S. Pispas, Thin films of PS/PS-b-PNIPAM and PS/PNIPAM polymer blends with tunable wettability. J. Polym. Sci. Part B **57**, 670–679 (2019)
7. A.V. Rudakova, A.V. Emeline, Photoinduced hydrophilicity of surfaces of thin films. Colloid J **83**, 20–48 (2021)
8. X. Deng, J.L. Livingston, N.J. Spear, G.K. Jennings, pH-responsive copolymer films prepared by surface-initiated polymerization and simple modification. Langmuir **36**, 715–722 (2020)
9. F. Ofridam, M. Tarhini, N. Lebaz, E. Gagniere, D. Mangin, A. Elaissari, pH-sensitive polymers: Classification and some fine potential applications. Polym. Adv. Technol. **32**, 1455–1484 (2021)
10. P. Roy, S. Ujjain, S. Dattatreya, S. Kumar, R. Pant, K. Khare, Mechanically tunable single-component soft polydimethylsiloxane (PDMS)-based robust and sticky superhydrophobic surfaces. Appl. Phys. A **125**, 535 (2019)
11. L. Hu, L. Hu, J. Wang, Z. Wang, F. Li, J. She, Y. Zhou, Y. Zhang, Y. Liu, Mechanical response of surface wettability of Janus porous membrane and its application in oil-water separation. Nanotechnology **33**, 245704 (2022)
12. X. Gao, Z. Guo, Biomimetic superhydrophobic surfaces with transition metals and their oxides: A review. J. Bionic Eng. **14**, 401–439 (2017)
13. L. Chen, W. Wang, B. Su, Y. Wen Y, C. Li, Y. Zhou, M. Li, X. Shi, H. Du, Y. Song, L. Jiang, A light-responsive release platform by controlling the wetting behavior of hydrophobic surface, ACS Nano 8, 744–751 (2014).
14. Z. Cheng, H. Lai, N. Zhang, K. Sun, L. Jiang, Magnetically induced reversible transition between Cassie and Wenzel states of superparamagnetic microdroplets on highly hydrophobic silicon surface. J. Phys. Chem. C **116**, 18796–18802 (2012)
15. S. Parvate, P. Dixit, S. Chattopadhyay, Superhydrophobic surfaces: insights from theory and experiments. J. Phys. Chem. B **124**, 1323–1360 (2020)
16. X. Luo, Z. Zhu, Y. Tian, J. You, L. Jiang, Titanium Dioxide Derived Materials with Superwettability. Catalysts **11**, 425 (2021)
17. J. Pan, S.J. Zhang, H. Shen, Q. Xiong, S. Mathur, Switchable Wettability in SnO_2 Nanowires and SnO_2@SnO_2 Heterostructures. J. Phys. Chem. C **116**, 13835–13836 (2012)
18. M. Alexiadou, M. Kandyla, G. Mousdis, M. Kompitsas, Pulsed laser deposition of ZnO thin films decorated with Au and Pd nanoparticles with enhanced acetone sensing performance. Appl. Phys. A **123**, 262 (2017)
19. M.A. Borysiewicz, ZnO as a Functional Material, a Review. Curr. Comput.-Aided Drug Des. **9**, 505 (2019)
20. J. Sun, N. Li, L. Dong, X. Niu, M. Zhao, Z. Xu, H. Zhou, C. Shan, C. Pan, Interfacial-engineering enhanced performance and stability of ZnO nanowire-based perovskite solar cells. Nanotechnology **32**, 475204 (2021)
21. J. Sun, Q. Hua, R. Zhou, D. Li, W. Guo, X. Li, G. Hu, C. Shan, Q. Meng, L. Dong, C. Pan, Z.L. Wang, Piezo-phototronic effect enhanced efficient flexible perovskite solar cells. ACS Nano **13**, 4507–4513 (2019)
22. J. Wu, J. Chen, J. Xia, W. Lei, B. Wang, A Brief review on bioinspired ZnO superhydrophobic surfaces: theory, synthesis, and applications. Adv. Mater. Sci. Eng. **2013**, 232681 (2013)
23. E. Velayi, R. Norouzbeigi, Annealing temperature dependent reversible wettability switching of micro/nano structured ZnO superhydrophobic surfaces. Appl. Surf. Sci. **441**, 156–164 (2018)
24. G. Kwak, M. Seol, Y. Tak, K. Yong, Superhydrophobic ZnO nanowire surface: chemical modification and effects of UV irradiation. J. Phys. Chem. C **113**, 12085–12089 (2009)
25. H. Luo, J. Ma, P. Wang, J. Bai, G. Jing, Two-step wetting transition on ZnO nanorod arrays. Appl. Surf. Sci. **347**, 868–874 (2015)
26. S. Baruah, J. Dutta, Hydrothermal growth of ZnO nanostructures. Sci. Technol. Adv. Mater. **10**, 013001 (2009)
27. S. Guillemin, V. Consonni, E. Appert, E. Puyoo, L. Rapenne, H. Roussel, Critical nucleation effects on the structural relationship between ZnO seed layer and nanowires. J. Phys. Chem. C **116**, 25106–25111 (2012)
28. E.L. Papadopoulou, M. Barberoglou, V. Zorba, A. Manousaki, A. Pagkozidis, E. Stratakis, C. Fotakis, Reversible Photoinduced Wettability Transition of Hierarchical ZnO Structures. J. Phys. Chem. C **113**, 2891–2895 (2009)
29. M.A. Frysali, L. Papoutsakis, G. Kenanakis, S.H. Anastasiadis, Functional Surfaces with Photocatalytic Behavior and Reversible Wettability: ZnO Coating on Silicon Spikes. J. Phys. Chem. C **119**, 25401–25407 (2015)

30. C. Liu, Q. Zhang, T. Li, Z. Li, Sticky and slippy: Two hydrophobic states transition of ZnO, hierarchical films by fluoroalkylsilane modification. Int. J. Mod. Phys. B **23**, 1867–1872 (2009)
31. B. Bhushan, M. Novovsky, The rose petal effect and the modes of superhydrophobicity. Phil. Trans. R. Soc. A **368**, 4713–4728 (2010)
32. K. Sasmal, C. Mondal, A. Kumar Sinha, S. Sona Gauri, J. Pal, T. Aditya, M. Ganguly, S. Dey, T. Pal, Fabrication of Superhydrophobic Copper Surface on Various Substrates for Roll-off, Self-Cleaning, and Water/Oil Separation, ACS Appl. Mater. Interfaces 6, 22034–22043 (2014).
33. S. Sutha, S.C. Vanithakumari, R.P. George, U. Kamachi Mudali, Baldev Raj, K. R. Ravi, Studies on the influence of surface morphology of ZnO nail beds on easy roll off of water droplets, Appl. Surf. Sci. 347, 839–848 (2015).
34. S. Latthe, C. Terashima, K. Nakata, A. Fujishima, Superhydrophobic surfaces developed by mimicking hierarchical surface morphology of lotus leaf. Molecules **19**, 4256–4283 (2014)
35. N.P. Klochko, V.A. Barbash, K.S. Klepikova, V.R. Kopach, O.V. Yashchenko, D.O. Zhadan, S.I. Petrushenko, S.V. Dukarov, V.M. Sukhov, A.L. Khrypunova, Highly hydrophobic surfaces with rose petal-effect based on nanocellulose films coated by nanostructured CuI layers. Cellulose **28**, 9395–9412 (2021)
36. Y. Shao, J. Zhao, Y. Fan, Z. Wan, L. Lu, Z. Zhang, W. Ming, L. Ren, Shape memory superhydrophobic surface with switchable transition between "Lotus Effect" to "Rose Petal Effect." Chem. Eng. J. **382**, 122989 (2020)
37. D.L. Lai, G. Kong, X.C. Li, C.S. Che, Corrosion resistance of ZnO nanorod superhydrophobic coatings with rose petal effect or lotus leaf effect. J. Nanosci. Nanotechn. **19**, 3919–3928 (2019)
38. C. Li, M. Li, Z. Ni, Q. Guan, B.R.K. Blackman, E. Saiz, Stimuli-responsive surfaces for switchable wettability and adhesion. J. R. Soc. Interface **8**, 20210162 (2021)
39. C. Florica, N. Preda, M. Enculescu, I. Zgura, M. Socol, I. Enculescu, Superhydrophobic ZnO networks with high water adhesion. Nanoscale Res. Lett. **9**, 385 (2014)
40. K. Ichimura, S.K. Oh, M. Nakagawa, Light-Driven Motion of Liquids on a Photoresponsive Surface. Science **288**, 1624–1626 (2000)
41. M.K. Chaudhury, A. Chakrabarti, T. Tibrewal, Coalescence of drops near a hydrophilic boundary leads to long range directed motion. Extreme Mech. Lett. **1**, 104–113 (2014)
42. A. Shastry, M.J. Case, K.F. Bohringer, Directing droplets using microstructured surfaces. Langmuir **22**, 6161–6167 (2006)
43. J.E.Y. Jin, Y. Deng, W. Zuo, X. Zhao, D. Han, Q. Peng, Z. Zhang, Wetting models and working mechanisms of typical surfaces existing in nature and their application on superhydrophobic surfaces: a review. Adv. Mat. Interfaces **5**, 1701052 (2018)
44. Y. Tak, K. Yong, Controlled growth of well-aligned ZnO nanorod array using a novel solution method. J. Phys. Chem. B **109**, 19263–19269 (2005)
45. F. Xia, Y. Zhu, L. Feng, L. Jiang, Smart responsive surfaces switching reversibly between super-hydrophobicity and super-hydrophilicity. Soft Matter **5**, 275–281 (2009)
46. J. Zhang, Y. Liu, Z. Wei, J. Zhang, Mechanism for wettability alteration of ZnO nanorod arrays via thermal annealing in vacuum and air. Appl. Surf. Sci. **265**, 363–368 (2013)
47. J. Li, Q. Sun, S. Han, J. Wang, Z. Wang, C. Jin, Reversibly light-switchable wettability between superhydrophobicity and super-hydrophilicity of hybrid ZnO/bamboo surfaces via alternation of UV irradiation and dark storage. Progr. Org. Coat. **87**, 155–160 (2015)
48. D.G. Kotsifaki, M. Kandyla, P.G. Lagoudakis, Near-field enhanced optical tweezers utilizing femtosecond-laser nanostructured substrates. Appl. Phys. Lett. **107**, 211111 (2015)
49. M. Kanidi, A. Dagkli, N. Kelaidis, D. Palles, S. Aminalragia-Giamini, J. Marquez-Velasco, A. Colli, A. Dimoulas, E. Lidorikis, M. Kandyla, E.I. Kamitsos, Surface-enhanced raman spectroscopy of graphene integrated in plasmonic silicon platforms with three-dimensional nanotopography. J. Phys. Chem. C **123**, 3076–3087 (2019)
50. Y.M. Park, M. Gang, Y.H. Seo, B.H. Kim, Artificial petal surface based on hierarchical micro- and nanostructures. Thin Solid Films **520**, 362–367 (2011)
51. M.T.Z. Myint, N.S. Kumar, G.L. Hornyak, J. Dutta, Hydrophobic/hydrophilic switching on zinc oxide micro-textured surface. Appl. Surf. Sci. **264**, 344–348 (2013)
52. F. Li, G. Feng, X. Yang, C. Lu, G. Ma, X. Li, W. Xue, H. Sun, Tunable wettability pattern transfer photothermally achieved on zinc with microholes fabricated by femtosecond laser. Micromachines **12**, 547 (2021)
53. T. Hao, X. Ma, Z. Lan, N. Li, Y. Zhao, H. Ma, Effects of hydrophilic surface on heat transfer performance and oscillating motion for an oscillating heat pipe. Int. J. Heat Mass Transf. **72**, 50–65 (2014)
54. X. Liu, F. Yang, J. Guo, J. Fu, Z. Guo, New insight about unusual droplets: from mediating wettability to manipulate locomotion modes. Chem. Comm. **56**, 14757–14788 (2020)